

1215 cm⁻¹. Compound **16a** was unstable and correct analytical data could not be obtained.

Further experimental details can be found in the Supporting Information.

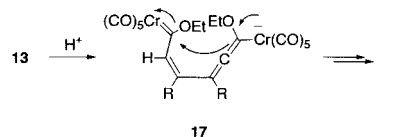
Received: March 5, 2002

Revised: June 6, 2002 [Z18826]

- [1] Selected reviews on the chemistry of metal carbene (Fischer) complexes: a) K. H. Dötz, H. Fischer, P. Hofmann, F. R. Kreissel, U. Schubert, K. Weiss, *Transition Metal Carbene Complexes*, Verlag Chemie, Deerfield Beach, FL, **1983**; b) K. H. Dötz, *Angew. Chem.* **1984**, 96, 573; *Angew. Chem. Int. Ed. Engl.* **1984**, 23, 587; c) W. D. Wulff in *Comprehensive Organic Synthesis*, Vol. 5 (Eds.: B. M. Trost, I. Fleming), Pergamon, Oxford, **1991**, p. 1065; d) L. S. Hegehus in *Comprehensive Organometallic Chemistry II*, Vol. 12 (Eds.: E. W. Abel, F. G. A. Stone, G. Wilkinson), Pergamon, Oxford, **1995**, p. 549; e) D. F. Harvey, D. M. Sigano, *Chem. Rev.* **1996**, 96, 271; f) J. Barluenga, F. J. Fañanás, *Tetrahedron* **2000**, 56, 4597; g) M. A. Sierra, *Chem. Rev.* **2000**, 100, 3591.
- [2] P. J. Krusic, U. Klabunde, C. P. Casey, T. F. Block, *J. Am. Chem. Soc.* **1976**, 98, 2015.
- [3] S. Lee, N. J. Cooper, *J. Am. Chem. Soc.* **1990**, 112, 9419.
- [4] K. Fuchibe, N. Iwasawa, *Org. Lett.* **2000**, 2, 3297.
- [5] Reviews: a) A. de Meijere, H. Schirmer, M. Duetsch, *Angew. Chem.* **2000**, 112, 4124; *Angew. Chem. Int. Ed.* **2000**, 39, 3964; b) R. Aumann, H. Nienaber, *Adv. Organomet. Chem.* **1997**, 41, 163.
- [6] a) M. Gómez-Gallego, M. J. Mancheño, P. Ramírez, C. Piñar, M. A. Sierra, *Tetrahedron* **2000**, 56, 4893; b) M. J. Mancheño, M. A. Sierra, M. Gómez-Gallego, P. Ramírez, *Organometallics* **1999**, 18, 3252.
- [7] For related rearrangements with other simple nucleophiles see: a) J. Barluenga, E. Rubio, J. A. López-Pelegrín, M. Tomás, *Angew. Chem.* **1999**, 111, 1163; *Angew. Chem. Int. Ed.* **1999**, 38, 1091. For additions of dihydropyridines see: b) H. Rudler, A. Parlier, B. Martín-Vaca, E. Garrier, J. Vaissermann, *Chem. Commun.* **1999**, 1439; c) H. Rudler, A. Parlier, V. Certal, J. Vaissermann, *Angew. Chem.* **2000**, 112, 3559; *Angew. Chem. Int. Ed.* **2000**, 39, 3417.
- [8] Reviews: a) R. Csuk, B. I. Glänzer, A. Fürstner, *Adv. Organomet. Chem.* **1988**, 28, 85; b) D. Savoia, C. Trombini, A. Umani-Ronchi, *Pure Appl. Chem.* **1985**, 57, 1887.
- [9] M. A. Schwindt, T. Lejon, L. S. Hegehus, *Organometallics* **1990**, 9, 2814.
- [10] Structure of **9a** was elucidated by X-ray crystallography. Crystal data: $M_r = 510.45$, orthorhombic, space group = $Pc2_1n$, $a = 10.174(4)$, $b = 12.653(3)$, $c = 19.559(9)$ Å, $V = 2517.9(16)$ Å³, $Z = 4$, $\rho = 1.349$ Mg m⁻³, $Mo_{K\alpha} = 0.71069$ Å, $\mu = 0.498$ mm⁻¹, $R = 0.0385$, $R_w = 0.1210$, 2315 reflections, 319 refined parameters; refinement on F^2 . The data were collected with an Enraf-Nonius CAD-4 diffractometer ($T = 298(2)$ K). The structure and the refinement of the crystal structure were done with the SHELX97 program. The non-hydrogen atoms were refined anisotropically. CCDC-180496 (**9a**) contains the supplementary crystallographic data for this paper. These data can be obtained free of charge via www.ccdc.cam.ac.uk/conts/retrieving.html (or from the Cambridge Crystallographic Data Centre, 12, Union Road, Cambridge CB2 1EZ, UK; fax: (+44) 1223-336-033; or deposit @ccdc.cam.ac.uk).
- [11] a) M. Contento, D. Savoia, C. Trombini, A. Umani-Ronchi, *Synthesis* **1979**, 30; For reductive dimerization of α,β -unsaturated esters see: b) J. Inanaga, Y. Handa, T. Tabuchi, K. Otsubo, M. Yamaguchi, T. Hanamoto, *Tetrahedron Lett.* **1991**, 32, 6557; c) K. Takaki, F. Beppu, S. Tanaka, Y. Tsubaki, T. Jintoku, Y. Fujiwara, *J. Chem. Soc. Chem. Commun.* **1990**, 516; d) I. Fussing, O. Hammerich, A. Hussain, M. Folmer Nielsen, J. H. P. Utley, *Acta Chem. Scand.* **1998**, 52, 328.
- [12] The percentages of deuterium incorporation in compounds **8e** and **9c** (> 99% in each case) were determined by ¹H NMR. For compound **9c** the percentages of deuteration were D³: 100% and D⁵: 70%.
- [13] The dimerization of chromium carbene α anions is known. a) L. Lattuada, E. Licandro, S. Maiorana, H. Molinari, A. Papagni, *Organometallics* **1991**, 10, 807; b) A. Geisbauer, S. Mihaan, W. Beck, *J. Organomet. Chem.* **1995**, 501, 61.
- [14] a) H.-P. Wu, R. Aumann, R. Fröhlich, B. Wibbeling, O. Kataeva, *Chem. Eur. J.* **2001**, 7, 5084; b) K. Ohe, T. Yokoi, K. Miki, F. Nishino, S.

Uemura, *J. Am. Chem. Soc.* **2002**, 124, 526; c) T. Miura, N. Iwasawa, *J. Am. Chem. Soc.* **2002**, 124, 518; For related cyclizations see: d) J. Barluenga, F. Aznar, S. Barluenga, M. Fernández, A. Martín, S. García-Granda, A. Piñera-Nicolás, *Chem. Eur. J.* **1998**, 4, 2280.

- [15] A reviewer has suggested an alternate mechanism. Monoprotonation of **13** would give intermediate **17** which by cyclization by the addition of the enolate anion of one carbene complex to the other neutral carbene would yield the final product **9**.



- [16] a) M. A. Sierra, M. J. Mancheño, E. Sáez, J. C. del Amo, *J. Am. Chem. Soc.* **1998**, 120, 6812; b) M. A. Sierra, J. C. del Amo, M. J. Mancheño, M. Gómez-Gallego, *J. Am. Chem. Soc.* **2001**, 123, 851.
- [17] Compounds **16** were unstable products and considerable loss of material was observed upon chromatographic purification.
- [18] R. Aumann, *Eur. J. Org. Chem.* **2000**, 17.
- [19] Complexes **6** and **7** were prepared by procedures previously described in the literature. a) **6a–d**: R. Aumann, H. Heinen, *Chem. Ber.* **1987**, 120, 537; b) **7a**: R. Aumann, P. Hinterding, *Chem. Ber.* **1993**, 126, 421; c) **7b**: I. Fernández, M. A. Sierra, M. J. Mancheño, M. Gómez-Gallego, S. Ricart, *Organometallics* **2001**, 20, 4304.

Probing Fast Facilitated Ion Transfer across an Externally Polarized Liquid–Liquid Interface by Scanning Electrochemical Microscopy**

Peng Sun, Zhiquan Zhang, Zhao Gao, and Yuanhua Shao*

Ion transfer reactions at a liquid–liquid interface or an interface between two immiscible electrolyte solutions are essential for many biological and chemical processes, such as transmembrane signaling, drug delivery, and phase-transfer catalysis.^[1–3] Over the last three decades, the thermodynamics and kinetics of such processes have been extensively studied using electrochemical methods. Several groups have tried to measure the rate constant using transient techniques,^[4] but met with limited success. This is mainly because the ion transfer is often very fast and therefore the transfer rate is difficult to measure.^[4]

Recently we obtained the rate constant of potassium ion transfer from water to 1,2-dichloroethane facilitated by dibenzo[18]crown-6 (DB18C6) using nanopipet voltammetry.

[*] Prof. Y. Shao, P. Sun, Z. Zhang, Z. Gao
State Key Laboratory of Electroanalytical Chemistry
Changchun Institute of Applied Chemistry
of the Chinese Academy of Sciences
Changchun 130022 (China)
Fax: (+86) 431-568-5653
E-mail: yhshao@ns.ciac.jl.cn

[**] This work was supported by the National Science Foundation of China (no. 2985111) and the Chinese Academy of Sciences. We thank Mr. L. Ge for his help in obtaining SEM images and Dr. Q. Wan (Tianjin University) for stimulating discussions.

try.^[5] This type of pipet provides a very high mass transfer rate and efficiently reduces an uncompensated drop in iR . Scanning electrochemical microscopy (SECM) is a powerful tool in the investigation of fast heterogeneous kinetics at liquid–solid and liquid–liquid interfaces, microfabrication, and imaging of local electrochemical reactivity.^[6] The use of a micropipet as the tip of the SECM instrument has shown promise for the imaging of various substrates, especially biological specimens.^[7–9]

Up to now, SECM studies on the kinetics of electron transfer across a liquid–liquid interface have been carried out at a nonpolarized liquid–liquid interface, where a common ion is employed in both phases to control the drop in potential across the interface.^[6–9] One limitation of this approach is that the adjustable potential differences are rather narrow (± 120 mV). However, most of the thermodynamic and kinetic data on charge transfer reactions have been obtained by using convenient electrochemical techniques to polarize and control the potential difference externally at such polarized liquid–liquid interfaces. The adjustable potential difference is limited by the potential window and is usually about 300 to 600 mV. We have recently applied SECM to study electron transfer reactions at a polarized liquid–liquid interface, based on a novel three-electrode setup that we developed.^[10,11]

To the best of our knowledge, SECM studies on the kinetics of facilitated ion transfer across an externally polarized interface have not been described in the literature. Here we report the kinetic measurements of K^+ transfer across the water–1,2-dichloroethane (W–DCE) interface facilitated by DB18C6 through the use of SECM with a nanopipet as the tip. As shown in Figure 1, an Ag/AgCl electrode is covered with a

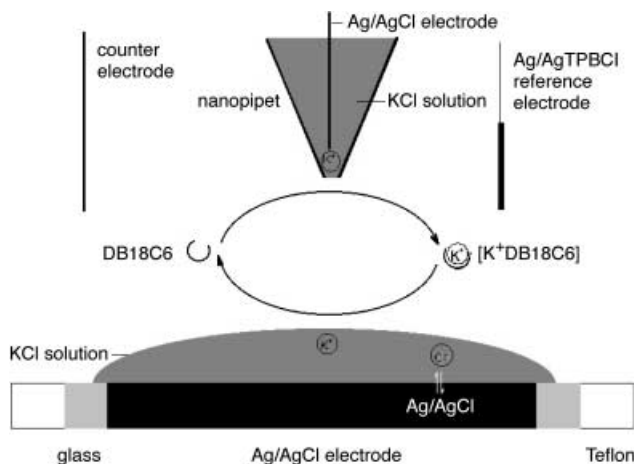


Figure 1. Schematic diagram of the application of SECM to probe facilitated ion transfer at an externally polarized liquid–liquid interface. TPBCL = tetrakis(4-chlorophenyl)borate.

droplet of aqueous KCl solution and immersed in the DCE phase. The Ag/AgCl electrode serves both as a counter and a reference electrode, and its potential remains constant as long as the concentration of KCl in the droplet is not changed.^[10] The W–DCE interface formed can be polarized externally by a three-electrode setup (the experimental setup shown in the lower part of Figure 1, where the SECM tip is not involved).

This assembly can be employed to study simple, facilitated ion and electron transfer reactions. The Ag/AgCl electrode is covered fully with 2 μ L of a 0.1 M KCl solution and immersed into 0.4 mL of a DCE solution; a phase volume ratio ($r = V_O/V_W$; V_O = volume of organic phase, V_W = volume of aqueous phase) of about 200 was used in all experiments. The area of this interface is about 0.009 cm², and well-defined voltammograms have been obtained for the three cases studied (Figure 2). Although the droplets are small and the size of

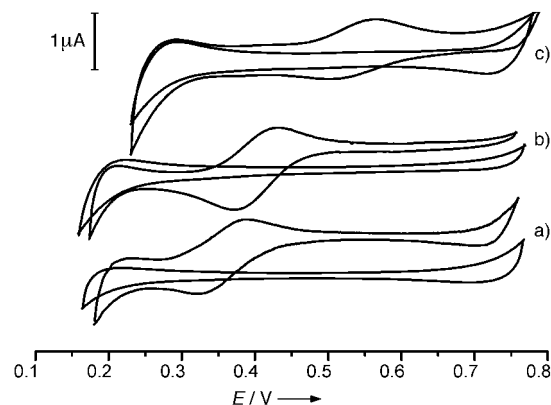


Figure 2. Cyclic voltammograms obtained for charge transfer reactions by use of a three-electrode setup. The potential E is given versus Ag/Ag(TPBCl). a) Potential window and facilitated K^+ transfer reaction. The cell consists of Ag/Ag(TPBCl)/10 mM TBA(TPBCl) + 0.25 mM DB18C6//100 mM KCl/AgCl/Ag; b) Potential window and electron transfer reaction. The cell consists of Ag/Ag(TPBCl)/10 mM TBA(TPBCl) + 0.2 mM TCNQ//1 M LiCl + 10 mM $K_3[Fe(CN)_6]$ + 400 mM $K_4[Fe(CN)_6]$ /AgCl/Ag; c) Potential window and TEA⁺ transfer reaction. The cell consists of Ag/Ag(TPBCl)/10 mM TBA(TPBCl)//100 mM LiCl + 0.4 mM TEACl/AgCl/Ag. TCNQ = 7,7,8,8-tetracyano-*p*-quinodimethane, TEA = tetraethylammonium.

the W–DCE interface formed is in the mm range, all of voltammograms are peak-shaped, indicating that the charge transfer reactions are controlled by a semi-infinite diffusion field. These results clearly indicate that this three-electrode setup works well as it simplifies the instrumentation used for studying charge transfer across liquid–liquid interfaces.

A nano-sized liquid–liquid interface can be formed at the nanorifice of the pipet between the bulk organic phase and the aqueous solution inside the nanopipet. The outer wall of the nanopipet was silanized prior to use.^[8c] A nearly perfect steady-state voltammogram can be obtained at the same potential as shown in Figure 2a.^[12] For the kinetic analysis, one needs to know the radius of the pipet a as well as the value of R_g ($R_g = r_g/a$, where r_g is the radius of the glass insulator plus the radius of the pipet). The latter can be estimated from SEM and is equal to 1.3. The radius of the pipet can be obtained either by SEM or by theoretical simulation. In our case, a value of 240 nm was determined from the SEM image of the pipet (Figure 3).

For comparison, we carried out the theoretical simulation as well, following the approach described in reference [8b]. The principle of this approach is to apply a theoretical equation with a certain value for R_g and calculate the radius of the pipet from an experimental cyclic voltammogram. We simulated the case of a nanopipet with $R_g = 1.3$ and obtained



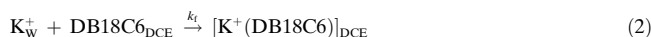
Figure 3. An SEM image of the pipet used in the experiments. Scale bar = 1 μm .

the steady-state limiting current (I), which can be represented by Equation (1), where n is the number of charge transferred,

$$I = 4.82 n F a D c^0 \quad (1)$$

F is the Faraday constant, a is the radius of the pipet, D is the diffusion coefficient, and c^0 is the bulk concentration of the ionophore. The concentration of K^+ in the aqueous phase is much higher than that of DB18C6 in the DCE phase, and the tip current is limited by diffusion of DB18C6 to the interface.^[8a] Assuming that the diffusion coefficient of DB18C6 in the DCE phase is $5.2 \times 10^{-6} \text{ cm}^2 \text{ s}^{-1}$,^[5] the effective radius of the nanopipet is found to be 238 nm, which is in good agreement with the value obtained by SEM.

The reactions in the system studied can be described by Equations (2) and (3). Reaction (2) takes place at the tip and



reaction (3) at the substrate. We chose this interfacial transfer reaction as a model system mainly because its mechanism is well established and attributed to transfer by interfacial complexation/transfer by interfacial dissociation (TIC/TID). In a typical SECM experiment, the tip is usually placed in a solution containing the oxidized (or reduced) form of a redox mediator, and this mediator is reduced (or oxidized) at the tip. If the tip is positioned close to an electrically conductive substrate, the species produced on the tip can diffuse to the substrate surface and in turn be re-oxidized (or re-reduced). This recycling produces an enhancement in the tip current (i_T) depending upon the distance d between the tip and the substrate; this is called positive feedback. For an insulating substrate, there is no recycling process and the substrate blocks the diffusion of the oxidized species to the tip. Thus i_T decreases at smaller d ; this is called negative feedback. The overall rate constant of mediator regeneration at the substrate can be evaluated from the tip current–distance curve (i_T – d), which is also referred to as an approach curve.

In our experiment, the recycling process is not the result of an electrochemically active mediator, but it is maintained by the TIC/TID mechanism. The tip is held at a potential E_T where the reaction in Equation (2) is diffusion-controlled.

Meanwhile, the potential difference E_S at the larger W–DCE interface (substrate) is externally controlled by a bipotentiostat to observe the effect of a polarized substrate on the transfer process at the tip (see Figure 1). The point of $d = 0$ can be precisely determined when the tip touches the substrate interface, which causes a sharp increase (or decrease) in the tip current.

Under our experimental conditions, the rate constant of the total interfacial reaction may be expressed by Equation (4),

$$k_\text{f} = k^\circ \exp[\alpha n f (E_\text{S} - E_\text{S}^0)] \quad (4)$$

where k° is the standard rate constant, α is the transfer coefficient, n is the number of charge transferred, E_S^0 is the formal potential, and $f = RT/nF$. When the value of $E_\text{S} - E_\text{S}^0$ becomes larger, k_f becomes smaller, and it becomes easier to obtain the kinetic parameter. Therefore the rate constant of this recycling can be adjusted by controlling the potential of this interface. When E_S is smaller than the half-wave potential $E_{1/2}$, the substrate functions approximately like a conducting substrate. The recycling shown in Figure 1 can be maintained.

From the experimental approach curves shown in Figure 4, we can determine the rate constants k_f by using the best fit of the experimental results with the theoretical values. The value

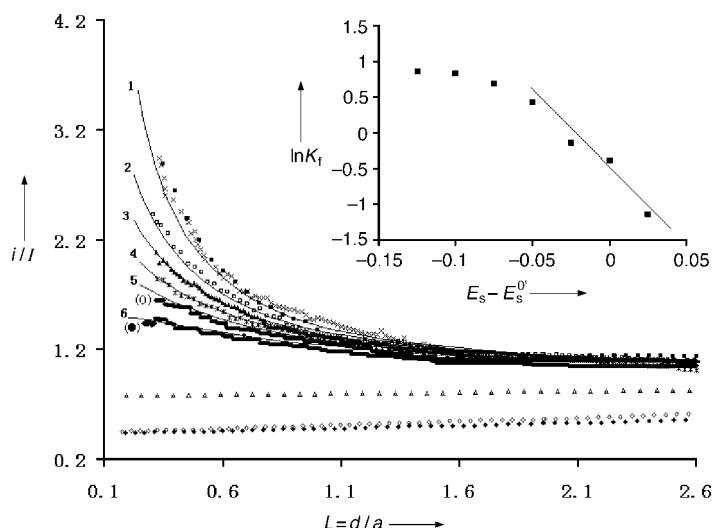


Figure 4. Experimental approach curves of a pipet with a 238 nm radius fitted with the theoretical values. The tip potential is 0.45 V, the substrate potential is 0.20 (■), 0.225 (×), 0.25 (□), 0.275 (▲), 0.30 (*), 0.325 (○), 0.35 (●), 0.375 (△), 0.40 (◇), and 0.425 V (◆). Curve 1 shows the theoretical curve for a diffusion-controlled process, and curves 2–6 are theoretical curves for kinetically controlled processes. Inset: the dependence of the heterogeneous rate constants on different values for E_S^0 .

of E_S^0 is evaluated from $E_{1/2}$ of the nernstian voltammograms,^[10a] and is equal to 0.325 V for Figure 2a. The values of k_f are in the range of 0.3–1.9 cm s^{-1} . The plot of $\ln k_\text{f}$ vs. E_S^0 is depicted in the inset of Figure 4. The values of k° and α can be evaluated from the intercept of the extrapolation and the slope of the plot, and are equal to $0.7 \pm 0.3 \text{ cm s}^{-1}$ and 0.56 ± 0.08 , respectively. These results are in good agreement with the values obtained by nanopipet voltammetry.^[5]

Let us now consider two limiting cases associated with the application of high negative and positive potentials. If more negative potentials are applied, the approach curves will overlap with the diffusion-controlled curves. In addition, the contribution of the transfer of supporting electrolyte will be significant. In such cases, the rate constants will be difficult to evaluate. When E_s is larger than $E_{1/2}$, most of the DB18C6 molecules in the DCE phase near the substrate exist as complexes with K^+ , and the concentration of free DB18C6 is close to zero. The recycling shown in Figure 1 cannot be maintained, and hence the substrate functions approximately like an insulating substrate. On the other hand, when the applied potentials at the substrate are larger than 0.35 V the experimental approach curves obtained deviate significantly from the theoretical ones. This is probably due to the fact that the substrate surface is positive under those conditions, preventing K^+ from diffusing to it. Consequently, the recycling is not maintained. The reaction shown in the Equation (3) can also be involved competitively, and thus the theoretical equations developed for fitting the experimental approach curves may be inadequate in this case.

Experimental Section

1,2-Dichloroethane (DCE, A.R.), potassium chloride (A.R.), and trimethylchlorosilane (A.R.) were obtained from Shanghai Chemical Co., China. Dibenzo[18]crown-6 (DB18C6, 98%) was purchased from Aldrich. Tetrabutylammonium tetrakis(4-chlorophenyl)borate (TBA-TPBCl) was synthesized according to published procedures,^[4d] and used as the supporting electrolyte in the organic phase. Millipore water was employed for the preparation of aqueous solutions.

A Model P-2000 laser puller (Sutter Instrument Co., USA) was used to prepare the pipet with an orifice radius in the range of 0.2–4 μm from borosilicate capillaries (1 mm outer diameter, 0.58 mm inner diameter). The outer walls of the pipets were silanized according to a described procedure.^[8c] A 0.1 M KCl solution was filled from the back using a 10- μL syringe. Silver wire (0.125 mm in diameter) coated with AgCl was inserted into the pipet as the reference electrode. The pipet was checked using an Olympus BX-60 optical microscope (BX-60, Olympus) prior to each measurement to ensure there was no bubble trapped inside. The R_g value of the pipets employed is about 1.3; this can be achieved by developing a suitable program and checked by a JXA-840 SEM (JEOL).

For experiments using the three-electrode setup with an Ag/AgCl electrode covered with an aqueous phase, silver wire (2 mm diameter) was first sealed in a glass tube (3 mm outer diameter, 2 mm inner diameter) and then mounted in Teflon. Precautions must be taken to prevent leakage from these electrodes. After the silver surface was polished, it was coated with a layer of AgCl by electrolysis. Since glass and silver are hydrophilic, whereas Teflon is hydrophobic, a stable aqueous droplet can form on the Ag/AgCl surface. The glass insulator can also prevent the organic bulk phase from coming into contact with the Ag/AgCl surface. The schematic representation of the three-electrode system is similar to that in ref. [10b]. Cyclic voltammograms were recorded using a bipotentiostat (CHI900, CH Instruments, USA).

The larger liquid–liquid interface as the substrate of SECM was formed between an Ag/AgCl electrode covered with 2 μL of a 0.1 M KCl solution and 0.4 mL of a DCE solution containing 0.01 M TBA-TPBCl and 0.25 mM DB18C6. A Ag/AgTPBCl wire (0.125 mm diameter) and a Pt wire (0.5 mm diameter) were used as the reference and counter electrodes, respectively. The interfacial potential differences at the substrate and the tip were controlled separately by the CHI900 bipotentiostat, and measured versus the Ag/AgTPBCl reference electrode in the DCE solution. The approach curve was obtained by moving the tip toward the substrate interface and by recording the tip current as a function of d .

Received: March 14, 2002 [Z18895]

- [1] a) B. Liu, M. V. Mirkin, *Anal. Chem.* **2001**, *73*, 670A–677A; b) F. Reymond, D. Fermin, H. Lee, H. H. Girault, *Electrochim. Acta* **2000**, *45*, 2647–2662; c) B. Liu, M. V. Mirkin, *Electroanalysis* **2000**, *12*, 1433–1447; d) I. Benjamin, *Chem. Rev.* **1996**, *96*, 1449–1475; e) A. G. Volkov, D. W. Deamer, *Liquid-Liquid Interfaces. Theory and Methods*, CRC, Boca Raton, **1996**; f) H. H. Girault in *Modern Aspects of Electrochemistry*, Vol. 25 (Eds.: J. O'M. Bockris, B. E. Conway, R. E. White), Plenum, New York, **1993**, p. 1; g) J. Koryta, *Electrochim. Acta* **1979**, *24*, 293–300.
- [2] a) A. G. Volkov, M. L. Gugeshashvili, D. W. Deamer, *Electrochim. Acta* **1995**, *40*, 2849–2868; b) A. G. Volkov, *Electrochim. Acta* **1998**, *44*, 139–153; c) H. H. Girault, D. J. Schiffrin, *J. Electroanal. Chem.* **1988**, *244*, 15–26; d) H. H. Girault, D. J. Schiffrin in *Charge and Field Effects in Biosystems* (Eds.: M. J. Allen, P. N. R. Usherwood), Abacus, Tunbridge Wells, **1996**, p. 171.
- [3] a) K. Arai, M. Ohasawa, F. Kusu, K. Takamura, *Bioelectrochem. Bioenerg.* **1993**, *31*, 65–73; b) I. M. Kolthoff, *Anal. Chem.* **1979**, *51*, 1R–22R.
- [4] a) P. D. Beattie, A. Delay, H. H. Girault, *J. Electroanal. Chem.* **1995**, *380*, 167–175; b) P. D. Beattie, A. Delay, H. H. Girault, *Electrochim. Acta* **1995**, *40*, 2961–2969; c) K. Tokuda, F. Kitamura, Y. Liao, M. Okuwaki, T. Ohasaka, *Proceedings of the International Seminar on Charge Transfer at Liquid/Liquid and Liquid/Membrane Interfaces* (Kyoto, 19–22 November 1996), Kyoto, **1996**, p. 7; d) Y. Shao, M. D. Osborne, H. H. Girault, *J. Electroanal. Chem.* **1991**, *318*, 101–109.
- [5] Y. Shao, M. V. Mirkin, *J. Am. Chem. Soc.* **1997**, *119*, 8103–8104.
- [6] a) *Scanning Electrochemical Microscopy* (Eds.: A. J. Bard, M. V. Mirkin), Marcel Dekker, New York, **2001**; b) A. J. Bard, F. Fan, M. V. Mirkin in *Electroanalytical Chemistry*, Vol. 18 (Ed.: A. J. Bard), Marcel Dekker, New York, **1994**, p. 244; c) A. J. Barker, M. Gonssalves, J. V. Macpherson, C. J. Slevin, P. R. Unwin, *Anal. Chim. Acta* **1999**, *385*, 223–240; d) A. J. Bard, F. Fan, J. Kwak, O. Lev, *Anal. Chem.* **1989**, *61*, 132–138.
- [7] a) C. Wei, A. J. Bard, G. Nagy, K. Toth, *Anal. Chem.* **1995**, *67*, 1346–1356; b) T. Solomon, A. J. Bard, *Anal. Chem.* **1995**, *67*, 2787–2790; c) S. Amemiya, A. J. Bard, *Anal. Chem.* **2000**, *72*, 4940–4948.
- [8] a) Y. Shao, M. V. Mirkin, *J. Electroanal. Chem.* **1997**, *439*, 137–143; b) Y. Shao, M. V. Mirkin, *J. Phys. Chem. B* **1998**, *102*, 9915–9921; c) Y. Shao, M. V. Mirkin, *Anal. Chem.* **1998**, *70*, 3155–3161.
- [9] Y. Selzer, D. Mandler, *J. Phys. Chem.* **2000**, *104*, 4903–4910.
- [10] a) S. Ulmeanu, H. J. Lee, D. J. Fermin, H. H. Girault, Y. Shao, *Electrochem. Commun.* **2001**, *3*, 219–223; b) V. Gobry, S. Ulmeanu, F. Reymond, G. Bouchard, P. Carrupt, B. Testa, H. H. Girault, *J. Am. Chem. Soc.* **2001**, *123*, 10684–10690.
- [11] Z. Zhang, Y. Yuan, P. Sun, B. Su, J. Guo, Y. Shao, H. H. Girault, *J. Phys. Chem. B* **2002**, *106*, 6713–6717.
- [12] The voltammogram is similar to that shown in Figure 1a of ref. [5], but is not shown here.